

Antireflection coating for quantum-well Bragg structures

Zhenshan Yang,^{1,*} J. E. Sipe,¹ N. H. Kwong,² R. Binder,² and Arthur L. Smirl³

¹*Department of Physics and Institute of Optical Sciences, University of Toronto, Toronto, Ontario, Canada M5S 1A7*

²*College of Optical Sciences, The University of Arizona, Tucson, Arizona 85721, USA*

³*Laboratory for Photonics and Quantum Electronics, 138 IATL, University of Iowa, Iowa City, Iowa 52242, USA*

*Corresponding author: zhenshan@physics.utoronto.ca

Received October 30, 2006; revised April 9, 2007; accepted April 12, 2007;

posted April 25, 2007 (Doc. ID 76533); published July 19, 2007

We develop a strategy to reduce large reflection losses from quantum-well Bragg structures through an anti-reflection coating technique. It is based on generalized refractive indices, which we call “effective coupling indices” (ECIs), that can be introduced to describe the coupling of light into quantum-well Bragg structures. For the example of a spectrally narrow band, which is relevant for slow-light applications, we clarify the dependence of the ECIs on the spectral bandwidth and discuss the relation between the ECIs and the group-velocity index. Numerical simulations of reflection spectra demonstrate the effectiveness of the ECI concept. © 2007 Optical Society of America

OCIS codes: 190.5970, 320.7130.

1. INTRODUCTION

Periodic optical structures and photonic crystals have been widely studied in the context of new and future generations of photonic devices. A possible classification of these structures distinguishes (conventional) nonresonant photonic crystals [1], in which light experiences a periodic modulation of the refractive index, from resonant photonic crystals. In the latter, light interacts strongly with periodically placed optical resonances, since the fundamental Bragg frequency ω_B , or a multiple integer of ω_B , is chosen to be close to the optical resonance frequency. One important example in this class is the quantum-well Bragg structure, in which the optical resonance is the lowest exciton resonance, at frequency ω_x , associated with the 1s heavy-hole exciton [2–6].

Due to their unique physical properties, quantum-well Bragg structures may play an increasingly important role in future device applications. One area where these systems are potentially useful is the slowing and storing of light. A main motivation for developing systems that allow for controlled slowdown and/or storing of light pulses is the need for optical delay lines and optical buffers in optical communication systems. We have recently explored conceptual strategies for slowing and trapping light in quantum-well Bragg structures [7,8]. Similar to other examples of one-dimensional resonant photonic-bandgap structures (see, e.g., [9,10]), quantum-well Bragg structures exhibit a spectrally very narrow polariton band, situated between the Bragg frequency and the optical resonance frequency. In [7,8], we call this polariton band the “intermediate band (IB).” The IB’s spectral width, and hence the group velocity of light in this band, can be externally manipulated and reduced to zero. This opens the possibility of deliberately stopping and releasing a light pulse propagating in this band.

While the mechanism for controlling light speed inside

the Bragg structure has been understood, for practical implementation the efficiency of light coupling from the outside (a uniform dielectric medium) into the Bragg structure must also be considered. We found in [7] that incident light spectrally within the IB suffers large reflection losses at the surface of the quantum-well Bragg structure. Minimizing these reflection losses is thus an important part of the overall light trapping scheme. This paper discusses in detail an antireflection (AR) strategy we have devised for this purpose.

Reducing surface reflection losses is also important for other periodic photonic structures. For example, this issue has recently attracted increasing attention in works on nonresonant two-dimensional photonic crystals [11–13], where the focus appears to be on minimizing out-of-plane reflection (Bragg diffraction). Momeni and Adibi [13] studied the antireflection effect of inserting a transitional lattice layer with optical properties (specifically the size of air holes) gradually interpolating between those of the photonic crystal and the outside uniform medium. Witzens *et al.* [12] studied the use of an interface of mode-matching multilayered grating, consisting of air holes, designed to reduce reflection by destructive interference. Both schemes were shown to be efficient.

The two broad classes of AR strategies, apodization and destructive interference, can also be considered for resonant photonic bandgap structures. In the specific case of a quantum-well Bragg structure, a gradual transition would make the system significantly longer. Since current crystal growth techniques still pose a serious limitation to the size of quantum-well Bragg structures (typical sizes are limited to roughly ~ 200 quantum wells), apodization does not seem to be an ideal candidate for the minimization of reflection losses. We have therefore taken an approach based on destructive interference of reflected waves. The main aim is thus to design AR coatings made

up of a small number of dielectric layers that can easily be grown on top of the quantum-well Bragg structure. Furthermore, it is important that the coating can be optimized for certain frequency regions (such as the narrow band that supports the slow light), even if the corresponding Bloch waves in the systems cannot be modeled by just a few plane-wave components (cf. [12]). To meet these criteria, we have developed an AR-coating strategy that is based on the following central question: can the coupling between the normal modes of the two media—plane waves in air and Bloch waves in the quantum-well Bragg structure—be treated as if the Bragg structure were a uniform medium with an effective (real) index of refraction, and, if so, what are the conditions and what is the value of this index of refraction? Once the condition for such a real index—we will call it an “effective coupling index” or ECI [14]—is found, one can apply the conventional AR-coating design of using $\lambda/4$ layers, well known from interfaces between two spatially homogeneous systems [15–17]. It is the purpose of this paper to give a detailed analysis of such ECIs, their mathematical properties, and their application to optimizing light entry into the IB.

In [7,8], we have already briefly introduced the concept of the AR coating of quantum-well Bragg structures, and we have shown its significant advantages for the purpose of slow-light propagation in the IB. But we did not present a comprehensive analysis of the ECI that would allow for a detailed understanding of the concept, and that would make it accessible for more general use in future generations of quantum-well Bragg structures or equivalent one-dimensional resonant photonic crystals. Reducing surface reflections is generally not a severe problem for one-dimensional nonresonant photonic crystals, but where it is needed, our strategy can also be applied.

This paper is organized as follows. In Section 2, we formulate the problem of designing an AR coating of quantum-well Bragg structures by introducing the concept of an ECI, which enables us to generalize conventional AR-coating techniques of interfaces between two spatially homogeneous media. In Section 3, we establish the quantitative definition of one ECI. In Section 4, we present a more detailed study of the characteristics of this ECI within the IB, such as the dependence of the ECI on the bandwidth of the IB; introduce a second ECI; and investigate the relation between the ECIs and the “group-velocity index” (GVI).

2. ANTIREFLECTION COATING FOR QUANTUM-WELL BRAGG STRUCTURES: GENERAL CONCEPT

A schematic of a quantum-well Bragg structure, which is a periodic array (taken to be in the z direction) of thin identical semiconductor quantum wells, with interwell spacing a , in a uniform dielectric background with refractive index n_b , is shown in Fig. 1. In this system, the optical resonance is due to the lowest exciton resonance of the quantum wells, which is the 1s heavy-hole exciton resonance at frequency ω_x . The Bragg resonance frequency ω_B is given by $\omega_B = \pi c / (n_b a)$, where c is the speed of light in vacuum. The eigenfunctions of the infinitely long system

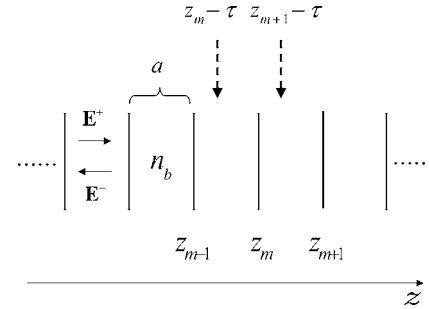


Fig. 1. Schematic of the quantum-well Bragg structure. The vertical solid lines represent infinitely thin identical quantum wells located at positions z_m and spaced by the distance a ; the background refractive index is n_b . The unit cell is defined to extend from $z_{m-1} - \tau$ to $z_{m+1} - \tau$. E^+ and E^- are the “forward” and “backward” traveling field components in the uniform medium between adjacent quantum wells, respectively.

can be written as Bloch waves that are labeled by a wave vector K and a band index ν ,

$$E(z, \omega) = u_{\nu, K}(z) e^{iKz}. \quad (1)$$

Here $\omega = \omega(\nu, K)$ is given by the photonic band structure of the system. Detailed expressions for the Bloch waves in our system are given by Yang *et al.* [7] and briefly reviewed in Appendix A.

A central problem for the design of an AR coating at the interface of a uniform (i.e., spatially homogeneous) medium and the Bragg structure is the fact that optical propagation is not fully described by simple plane waves. In a uniform (and nonabsorbing) medium characterized by the refractive index n , the eigenfunctions are plane waves, $E(z, \omega) = e^{iKz}$, and the dispersion relation is simply $\omega(K)n = cK$. This allows for the transfer matrix describing the interface between two uniform media to have simple matrix elements that are real and independent of space and wave vector. Before reviewing that transfer matrix, we want to outline the basic strategy for the case of a uniform-to-Bragg interface. In this case, one can try to generalize the dispersion relation with the help of an effective refractive index:

$$\omega(\nu, K)n_{\text{eff}} = cK, \quad (2)$$

with

$$\kappa = (1/i) \frac{d}{dz} \ln E(z, t). \quad (3)$$

This relation reduces trivially to the dispersion relation of a uniform medium with $\kappa = k$ and $n_{\text{eff}} = n$ if the waves are plane waves. But in the general case of Bloch waves, we see that κ is actually a nontrivial function, $\kappa = \kappa(\nu, K; z)$. This in turn means that $n_{\text{eff}} = n_{\text{eff}}(\nu, K; z)$. Depending on the z chosen, we find that n_{eff} can be real or complex. So one might ask whether or not such a quantity makes any physical sense. Yet, as we will find later in this paper, if z can be chosen so that n_{eff} is real, we can in fact generalize AR-coating techniques, well-known from uniform-to-uniform interfaces, to uniform-to-Bragg ones.

It will be useful to briefly review these uniform-to-uniform interfaces first. In Fig. 2(a), such an interface is schematically shown. The standard way to derive the

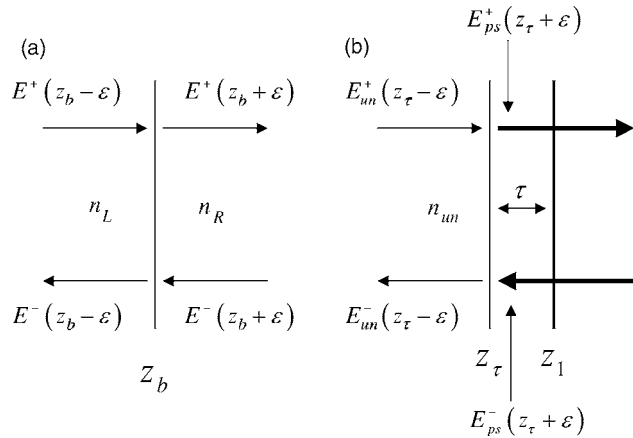


Fig. 2. (a) Boundary at z_b between two uniform media with refractive indices n_L on the left and n_R on the right. (b) A boundary at $z_\tau = z_1 - \tau$ between a uniform medium with refractive index n_{un} and a quantum-well Bragg structure as illustrated in Fig. 1; z_1 is the position of the first quantum well of the Bragg structure.

transfer matrix for a boundary between two uniform media, with refractive indices n_L on the left and n_R on the right, is to decompose the electric field into forward ($E^+ \propto e^{in_{LR}(\omega/c)z}$) and backward ($E^- \propto e^{-in_{LR}(\omega/c)z}$) traveling components [cf., Eq. (A1)]. Using the fact that the wave and its derivative are continuous at the boundary [i.e., using boundary conditions similar to those in Eq. (A2), except with z_m replaced by the location of the dielectric boundary z_b , and with $p_m = 0$], one finds

$$\begin{pmatrix} E^+(z_b - \varepsilon, \omega) \\ E^-(z_b - \varepsilon, \omega) \end{pmatrix} = \begin{bmatrix} \frac{n_R + n_L}{2n_L} & \frac{n_R - n_L}{2n_L} \\ \frac{n_R - n_L}{2n_L} & \frac{n_R + n_L}{2n_L} \end{bmatrix} \begin{pmatrix} E^+(z_b + \varepsilon, \omega) \\ E^-(z_b + \varepsilon, \omega) \end{pmatrix}, \quad \varepsilon \rightarrow 0^+. \quad (4)$$

The reflection and transmission (from left to right) can be obtained by setting $E^-(z_b + \varepsilon, \omega) = 0$ in Eq. (4) and solving for $r = -E^-(z_b - \varepsilon, \omega)/E^+(z_b - \varepsilon, \omega)$ and $t = E^+(z_b + \varepsilon, \omega)/E^+(z_b - \varepsilon, \omega)$:

$$r = \frac{n_L - n_R}{n_L + n_R}, \quad t = \frac{2n_L}{n_L + n_R}. \quad (5)$$

Equation (5) says that the reflection is determined by the mismatch of n_L and n_R (i.e., a larger mismatch means a larger reflection). It is well known that at any given frequency ω , the reflection from this boundary can be reduced to zero by adding one or more dielectric coating layers of optical thickness of $\lambda/4$ between the two media. Usually the reflection is also low in a spectral neighborhood of ω . The general requirement for the dielectric coating layers is as follows: with N coating layers between two uniform media with refractive indices n_0 and n_f , with the spatial sequence being $n_0 \rightarrow n_1 \rightarrow n_2 \rightarrow \dots \rightarrow n_{N-1} \rightarrow n_N \rightarrow n_f$, the refractive indices need to satisfy

$$n_0 \times \prod_{j=1}^N (n_j^2)^{(-1)^j} \times (n_f)^{(-1)^{N+1}} = 1. \quad (6)$$

Equation (6) can be proved by simply multiplying the transfer matrices in Eq. (4) for all the boundaries between

n_0 and n_f , together with the propagation matrices $\text{diag}(i, -i)$ between two adjacent boundaries (in the correct order).

The basic idea for applying the concept of an AR coating to the boundary between a uniform medium with refractive index n_0 and a quantum-well Bragg structure is to treat the latter structure as a uniform medium with an effective coupling index n_{eff} . The electric field in the Bragg structure is decomposed into its Bloch eigenfunctions ($E^\pm \propto u_{\nu, \pm K} e^{\pm iKz}$), and on the uniform medium side the decomposition is carried out in the usual way, i.e., $E^\pm \propto e^{\pm in_0(\omega/c)z}$. As we will see in the later sections, if we can choose z such that n_{eff} is real, then the transfer matrix for this uniform-to-Bragg boundary takes the same form as that in Eq. (4), only with n_R replaced by n_{eff} . Then we can identify this n_{eff} as the ‘‘effective coupling index’’ for the quantum-well Bragg structure and apply it to the AR-coating scheme by simply replacing n_f by n_{eff} in Eq. (6) to get the proper refractive indices of the coating layers.

3. EFFECTIVE COUPLING INDEX OF QUANTUM-WELL BRAGG STRUCTURES

In this section, we will establish a rigorous mathematical formula for the ECI in photonic bands for the quantum-well Bragg structure and discuss some of its general properties. A more specific study of the ECI in the IB (i.e., the spectrally narrow band that can be used for slow-light applications) is left to the next section.

Consider a boundary at $z_\tau = z_1 - \tau$ between a periodic quantum-well Bragg structure on the right and a uniform medium of refractive index n_{un} on the left [Fig. 2(b)]. Here z_1 is the position of the first quantum well and $0 \leq \tau \leq a$. At a given frequency ω within one of the photonic bands ν , the electric field on the left (uniform medium) is decomposed in the usual way as

$$E_{un}(z) = E_{un}^+(z) - E_{un}^-(z) = A_{un} e^{in_{un}(\omega/c)z} - B_{un} e^{-in_{un}(\omega/c)z} \quad \text{for } z < z_\tau, \quad (7)$$

where the subscript ‘‘un’’ stands for ‘‘uniform medium.’’ On the right (Bragg structure), the field is decomposed into the two Bloch eigenfunctions of the Bragg structure at frequency ω :

$$E_{ps}(z) = E_{ps}^+(z) - E_{ps}^-(z) = A_{ps} u_{\nu, K}(z) e^{iKz} - B_{ps} u_{\nu, -K}(z) e^{-iKz} \quad \text{for } z > z_\tau, \quad (8)$$

where the subscript ps means ‘‘periodic structure.’’ In Eq. (8), we assume that the K component $u_{\nu, K}(z) e^{iKz}$ corresponds to a net energy flow in the forward direction, i.e., $|E_0^+(\nu, K; \tau)/E_0^-(\nu, K; \tau)| > 1$, and the $-K$ component in the backward direction, i.e., $|E_0^+(\nu, -K; \tau)/E_0^-(\nu, -K; \tau)| < 1$, where $E_0^{\pm}(\nu, K; \tau)$ is the forward-backward component of the eigenvector of the unit cell transfer matrix $\bar{M}(\omega, \tau)$, corresponding to the eigenvalue e^{iKa} . For the rigorous definitions of these quantities, see Eqs. (A6)–(A10) of Appendix A.

In what follows, we will derive the transfer matrix relating $[E_{un}^+(z_\tau - \varepsilon), E_{un}^-(z_\tau - \varepsilon)]^T$ to $[E_{ps}^+(z_\tau + \varepsilon), E_{ps}^-(z_\tau + \varepsilon)]^T$ and cast it into a form analogous to that in Eq. (4). In this

way, we can quantitatively define and analyze the ECI of the quantum-well Bragg structure for some particular τ .

By substituting Eqs. (7) and (8) into the boundary conditions in Eq. (A2), with z_m replaced by $z_\tau = z_1 - \tau$, and with $p_m = 0$, after some straightforward algebra, we obtain

$$\begin{pmatrix} E_{un}^+(z_\tau - \varepsilon) \\ E_{un}^-(z_\tau - \varepsilon) \end{pmatrix} = \begin{bmatrix} \frac{n_{ps}^{(1)}(\nu, K; \tau) + n_{un}}{2n_{un}} & \frac{n_{ps}^{(2)}(\nu, K; \tau) - n_{un}}{2n_{un}} \\ \frac{n_{ps}^{(1)}(\nu, K; \tau) - n_{un}}{2n_{un}} & \frac{n_{ps}^{(2)}(\nu, K; \tau) + n_{un}}{2n_{un}} \end{bmatrix} \times \begin{pmatrix} E_{ps}^+(z_\tau + \varepsilon) \\ E_{ps}^-(z_\tau + \varepsilon) \end{pmatrix}, \quad (9)$$

with

$$n_{ps}^{(1)}(\nu, K; \tau) \equiv \frac{iKu_{\nu, K}(z_\tau + \varepsilon) + u'_{\nu, K}(z_\tau + \varepsilon)}{\frac{\omega}{c} - u_{\nu, K}(z_\tau + \varepsilon)}, \quad (10)$$

$$n_{ps}^{(2)}(\nu, K; \tau) \equiv \frac{iKu_{\nu, -K}(z_\tau + \varepsilon) - u'_{\nu, -K}(z_\tau + \varepsilon)}{\frac{\omega}{c} - u_{\nu, -K}(z_\tau + \varepsilon)}, \quad (11)$$

where $u' = \partial u / \partial z$. Furthermore, substituting Eq. (A15) into Eq. (11) gives

$$n_{ps}^{(2)}(\nu, K) = n_{ps}^{(1)*}(\nu, K), \quad (12)$$

so Eq. (9) can be rewritten as

$$\begin{pmatrix} E_{un}^+(z_\tau - \varepsilon) \\ E_{un}^-(z_\tau - \varepsilon) \end{pmatrix} = \begin{bmatrix} \frac{n_{ps}^{(1)}(\nu, K; \tau) + n_{un}}{2n_{un}} & \frac{n_{ps}^{(1)*}(\nu, K; \tau) - n_{un}}{2n_{un}} \\ \frac{n_{ps}^{(1)}(\nu, K; \tau) - n_{un}}{2n_{un}} & \frac{n_{ps}^{(1)*}(\nu, K; \tau) + n_{un}}{2n_{un}} \end{bmatrix} \times \begin{pmatrix} E_{ps}^+(z_\tau + \varepsilon) \\ E_{ps}^-(z_\tau + \varepsilon) \end{pmatrix}. \quad (13)$$

The transfer matrix in Eq. (13) does not yet have the same form as that for the dielectric boundary between two uniform media in Eq. (4), since it is not clear whether $n_{ps}^{(1)}(\nu, K; \tau)$ is real or not. However, for $\tau = a/2$ we will show below that $n_{ps}^{(1)}(\nu, K; a/2)$ is real for all frequencies in the photonic band ν , and the transfer matrix in Eq. (13) has exactly the same form as that in Eq. (4). Thus, the ECI can be defined as $n_{\text{eff}}(\omega) = n_{ps}^{(1)}(\nu, K; a/2)$. By simply replacing n_f in Eq. (6) with $n_{\text{eff}}(\omega)$, this ECI can be used to design AR coatings for uniform-to-Bragg boundaries, which reduces the reflection at the boundary to zero at $\omega = \omega(\nu, K)$. For any other τ , $0 \leq \tau \leq a$, an ECI can be so defined [i.e., $n_{ps}^{(1)}(\nu, K; \tau)$ is real] only at some particular frequencies.

To see how $\tau = a/2$ leads to a real $n_{\text{eff}}(\omega) = n_{ps}^{(1)}(\nu, K; a/2)$ in the photonic bands, we first express $n_{ps}^{(1)}(\nu, K; \tau)$ [Eq. (10)] in terms of $E_0^\pm(\nu, K; \tau)$ instead of $u_{\nu, K}(z_\tau + \varepsilon)$ and its derivative by use of Eq. (A11):

$$n_{ps}^{(1)}(\nu, K; \tau) = n_b \frac{\frac{E_0^+(\nu, K; \tau)}{E_0^-(\nu, K; \tau)} + 1}{\frac{E_0^+(\nu, K; \tau)}{E_0^-(\nu, K; \tau)} - 1}. \quad (14)$$

It is obvious from Eq. (14) that $n_{ps}^{(1)}(\nu, K; \tau)$ is real if and only if $E_0^+(\nu, K; \tau)/E_0^-(\nu, K; \tau)$ is real; on the other hand, from Eq. (A13) we see that $E_0^+(\nu, K; \tau)/E_0^-(\nu, K; \tau)$ is real at $\tau = a/2$ for all frequencies within the photonic bands; thus $n_{ps}^{(1)}(\nu, K; \tau)$ is real and can be defined as the ECI of the quantum-well Bragg structure,

$$n_{\text{eff}}(\omega) = n_{ps}^{(1)}\left(\nu, K; \frac{a}{2}\right) = n_b \frac{\frac{E_0^+\left(\nu, K; \frac{a}{2}\right)}{E_0^-\left(\nu, K; \frac{a}{2}\right)} + 1}{\frac{E_0^+\left(\nu, K; \frac{a}{2}\right)}{E_0^-\left(\nu, K; \frac{a}{2}\right)} - 1}. \quad (15)$$

To get a better idea how n_{eff} varies with frequency, we present some numerical results here. We consider a quantum-well Bragg structure with the following parameters:

$$\begin{aligned} \hbar\omega_x &= 1.4966 \text{ eV}, & \hbar\omega_B &= 1.4970 \text{ eV}, & n_b &= 3.61, \\ \Gamma &= 1.8 \times 10^{-5}, \end{aligned} \quad (16)$$

where Γ , defined in Eq. (A5), describes the strength of the coupling between the light field and the excitonic polarization. Also, as mentioned in Appendix A, the polarization nonradiative decay rate γ in Eq. (A3) is set to zero throughout this paper. The band structure of an infinite system near the Bragg resonance frequency ω_B , calculated from Eq. (A9), is shown in Fig. 3, which includes three (upper, lower, and intermediate) bands and two bandgaps associated with the exciton resonance and the Bragg resonance. As mentioned above, the IB, approximately extending from ω_x to ω_B , is of particular interest in our previous schemes of the deliberate control and manipulation of light propagation [7,8].

In Fig. 4, we show n_{eff} as a function of frequency in the upper, lower, and intermediate bands; with parameters given in Eq. (16). The ECI in the upper and lower bands is larger than the background refractive index n_b and increases dramatically as the frequency approaches the band edges, while in the IB the ECI is smaller than n_b —actually much smaller than 1 in the current case—and decreases to 0 as the frequency approaches the band edges.

To relate the ECI shown in Fig. 4 to the physical properties of the system, we plot in Fig. 5 the reflection spectrum of a finite quantum-well Bragg structure with 1000 quantum wells and one cap layer of the background medium, with thickness $\tau = a/2$, on each end of the structure. The uniform medium before the front surface is the air ($n = 1$) and that after the back surface is a substrate of the

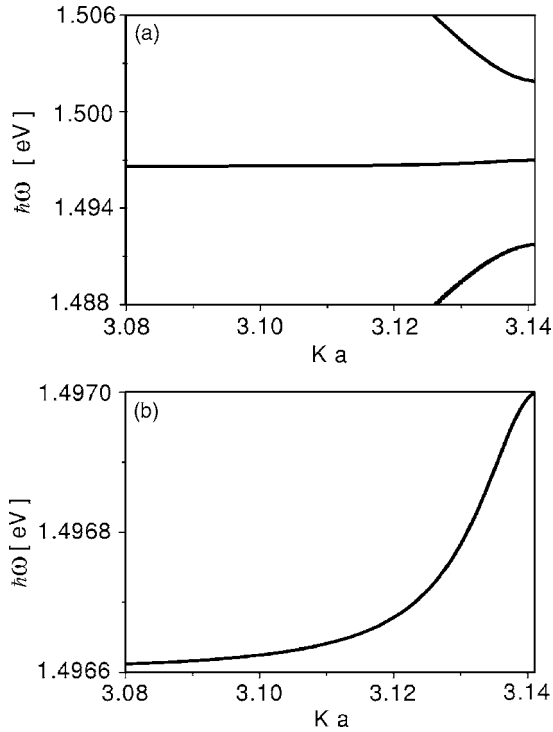


Fig. 3. Photonic band structure of the quantum-well Bragg structure specified in Eq. (16) near the Bragg resonance $\hbar\omega_B$ and exciton resonance $\hbar\omega_x$. (a) Large frequency scale, showing the upper and lower polariton band as well as the IB. (b) Extended view of the IB on a smaller frequency scale.

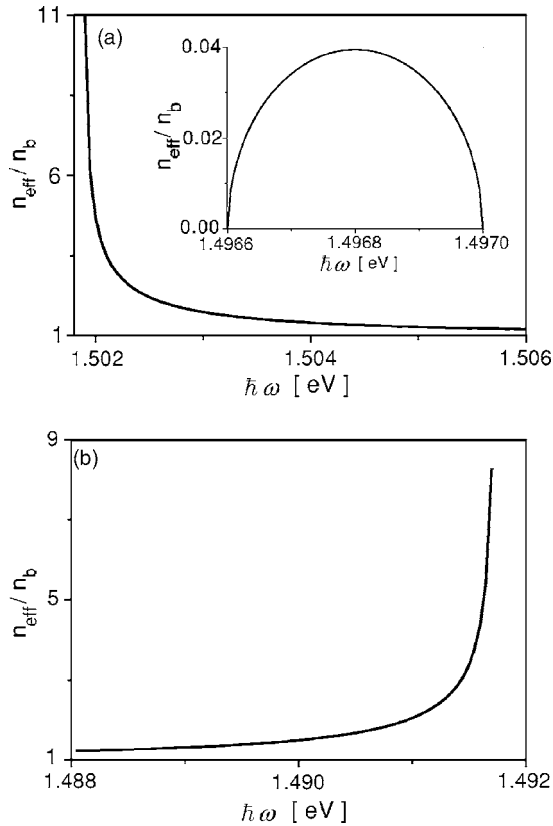


Fig. 4. ECI, n_{eff} , of the quantum-well Bragg structure as a function of $\hbar\omega$ in the (a) upper and (b) lower polariton band. The inset in (a) shows n_{eff} in the IB.

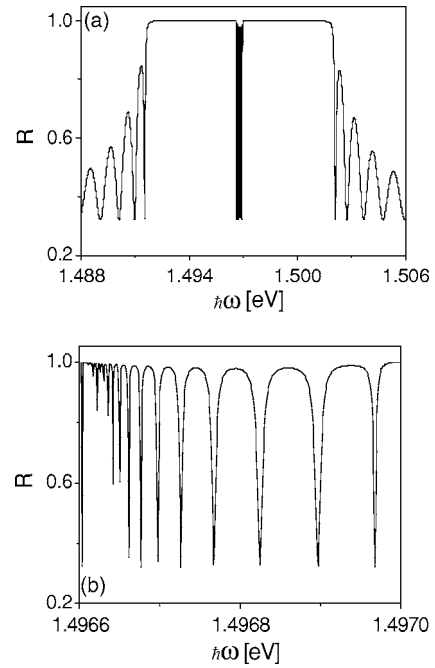


Fig. 5. (a) Reflection spectrum of the quantum-well Bragg structure without AR coating. (b) The same as (a) but restricted to the spectral region of the IB.

same material as the background medium (n_b); the other parameters are given in Eq. (16).

As expected, the reflectivity is unity within the bandgaps. In the intermediate band, the reflectivity is close to unity, except for sharp Fabry-Pérot-like features, which signal high reflectivity on both boundaries. In the slow-light applications discussed in [7,8], it is crucial to couple a light pulse spectrally located inside the IB from the air into the quantum-well Bragg structure, and back out (either transmitted or reflected) again. Thus it is necessary to reduce the reflection at both ends of the Bragg structure. To do this, we generalize the AR-coating scheme to the quantum-well Bragg structure simply by replacing n_f in Eq. (6) with the ECI at the given frequency (e.g., in the middle of the IB), where we want to make the reflection vanish. From Fig. 4, we estimate that in the middle of the IB, $n_{\text{eff}}/n_b \approx 0.04$. For this ECI, as an example we may choose an AR-coating layer sequence as “air $\rightarrow n=1.17 \rightarrow n=3.61 \rightarrow n=1.17 \rightarrow$ Bragg structure” on the air side and “Bragg structure $\rightarrow n=1.61 \rightarrow n=3.61 \rightarrow n=1.61 \rightarrow$ substrate” on the substrate side. [Note that Eq. (6) allows for various solutions regarding both the number of AR-coating layers and the values for the corresponding refractive indices.] The reflection spectrum of the quantum-well Bragg structure with these AR coatings is illustrated in Fig. 6; it clearly shows that the AR coatings dramatically reduce the reflection in the middle of the IB and its spectral neighborhood.

4. EFFECTIVE COUPLING INDEX IN THE INTERMEDIATE BAND

Due to the unique role played by the IB in slow-light applications, it is worth studying the characteristics of the ECI within the IB in more detail. In this section, we de-

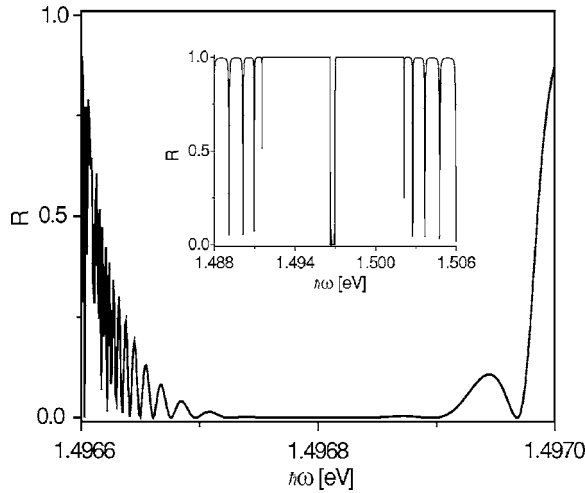


Fig. 6. Same as Fig. 5(a) [and the inset is the same as Fig. 5(b)], but for the case with AR coatings.

rive some simple but accurately approximate expressions for the ECI as a function of frequency within the IB. Qualitative features of the ECI, such as its relation to the IB bandwidth and the GVI, can be easily obtained with the aid of these approximate expressions.

In Eqs. (10) and (15), the ECI is defined in terms of the Bloch wave functions or the eigenvectors of the unit-cell transfer matrix, which in turn are complicated functions of ω , making it difficult to extract quantitative information on ECI from these formulas. It is thus helpful to derive a simpler formula for the ECI as an explicit function of ω .

For convenience, we first lay out some definitions and approximations for the IB situated between ω_x and ω_B , which will be used throughout the derivations:

$$\delta\omega_x \equiv \omega - \omega_x, \quad \delta\omega_B \equiv \omega - \omega_B, \quad \Delta\omega_{xB} \equiv \omega_x - \omega_B,$$

$$\beta = -i\Gamma \frac{\omega}{\omega - \omega_x} \approx -i\Gamma \frac{\omega_B}{\delta\omega_x} \equiv i \operatorname{Im} \beta, \quad (17)$$

$$\left| \frac{\delta\omega_x}{\omega_B} \right|, \left| \frac{\delta\omega_B}{\omega_B} \right| \ll 1, \quad \frac{1}{\pi \left| \frac{\delta\omega_B}{\omega_B} \right|} \gg |\beta| \gg \pi \left| \frac{\delta\omega_B}{\omega_B} \right|. \quad (18)$$

The approximations identified by Eq. (18) are usually well satisfied for the Bragg structures in which we are interested.

Taking $\tau = a/2$ in Eq. (A10), together with Eq. (A9), we have

$$\frac{E_0^+ \left(\nu, K; \frac{1}{2}a \right)}{E_0^- \left(\nu, K; \frac{1}{2}a \right)} = \frac{\operatorname{Im}[e^{i\pi(\omega/\omega_B)}(1 + i \operatorname{Im} \beta)] \pm \sqrt{1 - \{\operatorname{Re}[e^{i\pi(\omega/\omega_B)}(1 + i \operatorname{Im} \beta)]\}^2}}{\operatorname{Im} \beta}, \quad (19)$$

where we have used $\omega_B = \pi c/(n_b a)$. We have mentioned above that in the definition of $n_{\text{eff}}(\omega) = n_{ps}^{(1)}(\nu, K; a/2)$, K is assumed to be the value that makes $|E_0^+(\nu, K; a/2)/E_0^-(\nu, K; a/2)| > 1$. However, at this moment it is not clear which sign before the squared root in the numerator on the right-hand side of Eq. (19) corresponds to the right K , so we keep the \pm for now and will decide on the sign later.

To simplify Eq. (19), we expand $e^{i\pi(\omega/\omega_B)}$ to first order in $\delta\omega_B/\omega_B$:

$$e^{i\pi(\omega/\omega_B)} \approx -1 - i\pi \frac{\delta\omega_B}{\omega_B}, \quad (20)$$

which leads to

$$\begin{aligned} \frac{E_0^+ \left(\nu, K; \frac{1}{2}a \right)}{E_0^- \left(\nu, K; \frac{1}{2}a \right)} &\approx \frac{\left(\Gamma \frac{\omega_B}{\delta\omega_x} - \pi \frac{\delta\omega_B}{\omega_B} \right) \pm \sqrt{-2\pi\Gamma \frac{\delta\omega_B}{\delta\omega_x} - \left(-\pi\Gamma \frac{\delta\omega_B}{\delta\omega_x} \right)^2}}{-\Gamma \frac{\omega_B}{\delta\omega_x}}, \\ &\approx -1 - \sqrt{\left| \frac{2\pi \delta\omega_B \delta\omega_x}{\Gamma \omega_B \omega_B} \right|}, \end{aligned} \quad (21)$$

where we have chosen the appropriate sign before the squared root such that $|E_0^+(\nu, K; a/2)/E_0^-(\nu, K; a/2)| > 1$, and taken into account the fact that any ω within the IB is between ω_x and ω_B . The ECI in Eq. (15) is now simplified to

$$n_{\text{eff}}(\omega) \approx n_b \frac{\sqrt{\left| \frac{2\pi \delta\omega_B \delta\omega_x}{\Gamma \omega_B \omega_B} \right|}}{2 + \sqrt{\left| \frac{2\pi \delta\omega_B \delta\omega_x}{\Gamma \omega_B \omega_B} \right|}} \approx \frac{1}{2} n_b \sqrt{\frac{2\pi}{\Gamma} \left| \frac{\delta\omega_B}{\delta\omega_x} \right|} \times \left| \frac{\delta\omega_x}{\Delta\omega_{xB}} \right| \left| \frac{\Delta\omega_{xB}}{\omega_B} \right|. \quad (22)$$

We specify the frequency dependence of n_{eff} by writing it in terms of the ratios $|\delta\omega_B/\delta\omega_x|$, $|\delta\omega_x/\Delta\omega_{xB}|$, and $|\Delta\omega_{xB}/\omega_B|$ for a particular reason: under the approximations listed in Eq. (18), the IB is located close to ω_B and has a bandwidth approximately given by $|\Delta\omega_{xB}|$. Thus when comparing the ECIs in IBs with different bandwidths, it is natural to compare them at frequencies with the same $|\delta\omega_x/\Delta\omega_{xB}|$, i.e., at the same spectral position as scaled by the IB bandwidth. If we define $\alpha = |\delta\omega_x/\Delta\omega_{xB}|$, then $|\delta\omega_B/\Delta\omega_{xB}| = 1 - \alpha$ and $|\delta\omega_B/\delta\omega_x| = (1 - \alpha)/\alpha$, and α ranges from nearly 0 to 1 as the frequency varies within the IB. Equation (22) then shows that the ECI within the IB is proportional to the bandwidth of the IB. In the middle of the IB, $\alpha = 1/2$ and

$$n_{\text{eff}} \approx \frac{1}{2} n_b \sqrt{\frac{\pi}{2\Gamma} \left| \frac{\Delta\omega_{xB}}{\omega_B} \right|}. \quad (23)$$

In Fig. 7, we compare the two formulas for n_{eff} , rigorously given by Eq. (15) and approximately given by Eq. (22) in the IB, respectively. They are in excellent agreement.

We have mentioned that for $\tau = a/2$, the concept of the ECI, defined as $n_{ps}^{(1)}$ in Eqs. (10) or (15) when it is real, is valid for all frequencies in the photonic bands. For $\tau = a/2 + \Delta a$, $-a/2 \leq \Delta a \leq a/2$,

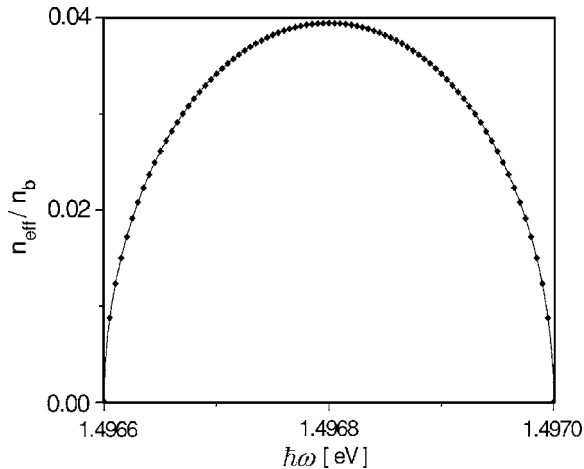


Fig. 7. ECI for $\tau = a/2$ given by the rigorous formula, Eq. (15), as functions of ω within the IB, shown as solid curve. The dots correspond to the approximate formula, Eq. (22).

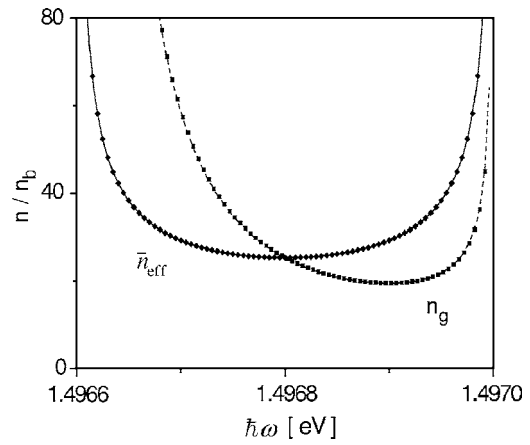


Fig. 8. ECI for $\tau = a$ and group-velocity index as functions of ω within the IB. The lines are based on the rigorous formulas: Eqs. (25) and (15) for the ECI, and $n_g = c|dK/d\omega|$ together with Eq. (A12) for the GVI. The dots are based on the approximate expressions, Eq. (26) for the ECI and Eq. (29) for the GVI.

$$\frac{E_0^+\left(\nu, K; \frac{a}{2} + \Delta a\right)}{E_0^-\left(\nu, K; \frac{a}{2} + \Delta a\right)} = e^{-2in_b(\omega/c)\Delta a} \frac{E_0^+\left(\nu, K; \frac{a}{2}\right)}{E_0^-\left(\nu, K; \frac{a}{2}\right)} \quad (24)$$

is real if and only if $e^{-2in_b(\omega/c)\Delta a} = \pm 1$. For IBs with the approximations in Eq. (18), when $\Delta a = a/2$ or $-a/2$ (i.e., $\tau = a$ or 0), $e^{-2in_b(\omega/c)\Delta a} \approx -1$, thus (using $\tau = a$ without loss of generality here and in the rest of this section, because $\tau = 0$ yields the same results) $E_0^+(\nu, K; a/2)/E_0^-(\nu, K; a/2) \approx -E_0^+(\nu, K; a/2)/E_0^-(\nu, K; a/2)$ is real to a good approximation. A real ECI can approximately also be defined, within the IB for $\tau = a$, by $\bar{n}_{\text{eff}}(\omega) \equiv n_{ps}(\nu, K; a)$, which can be shown to satisfy

$$\frac{\bar{n}_{\text{eff}}(\omega)}{n_b} = \frac{n_b}{n_{\text{eff}}(\omega)}, \quad (25)$$

i.e., $\bar{n}_{\text{eff}}(\omega)$ is inversely proportional to $n_{\text{eff}}(\omega)$. Substituting Eq. (22) into Eq. (25) gives

$$\bar{n}_{\text{eff}}(\omega) \approx 2n_b \sqrt{\frac{\Gamma}{2\pi} \left| \frac{\delta\omega_x}{\delta\omega_B} \right| \left| \frac{\Delta\omega_{xB}}{\delta\omega_x} \right| \left| \frac{\omega_B}{\Delta\omega_{xB}} \right|}, \quad (26)$$

showing that $\bar{n}_{\text{eff}}(\omega)$ is inversely proportional to the bandwidth of the IB. In Fig. 8, we plot \bar{n}_{eff} as a function of ω within the IB, also comparing the formula rigorously given by Eqs. (25) and (15) with the simplified version in Eq. (26), which again shows an excellent agreement, as expected.

Since the value of ECI is different for $\tau = a/2$ and $\tau = a$ (when $\omega \approx \omega_B$), the design of the AR coating for the boundary between a uniform medium of refractive index n_0 and a quantum-well Bragg structure is also different for $\tau = a/2$ and $\tau = a$, according to Eq. (6). In particular, a cap layer of a is equivalent to a cap layer of $a/2$ plus a $\lambda/4$ layer of the background index n_b [since $(n_b\omega/c) \times (a/2) \approx \pi/2$]. Thus the AR-coating layers for $\tau = a/2$ can be related to those for $\tau = a$ in a simple way: Suppose that for $\tau = a$, an AR coating is given by a $\lambda/4$ layer sequence of “uniform medium $\rightarrow n_1 \rightarrow n_2 \rightarrow \dots \rightarrow n_N \rightarrow$ Bragg structure.”

Then a $\lambda/4$ layer sequence of “uniform medium $\rightarrow n_1 \rightarrow n_2 \rightarrow \dots \rightarrow n_N \rightarrow n_b \rightarrow$ Bragg structure” is an appropriate AR coating for $\tau=a/2$. We note that, from a practical point of view, the AR coating for any structure with a cap layer different from $\tau=a$ (or $\tau=a/2$) can simply be designed by first adding one layer of index n_b that extends the existing cap layer to thickness a (or $a/2$), and then by using the design criteria given above for the respective cap layers of thickness a (or $a/2$).

We recall that in [7] the group velocity v_g in the IB is found to be proportional to the IB bandwidth, or equivalently, the GVI $n_g=c/v_g$ is inversely proportional to the bandwidth. It is thus instructive to see if there is any specific relation between the ECI and GVI [18].

Again we assume the approximations in Eq. (18). With the Taylor expansion in Eq. (20), the eigenvalue in Eq. (A12) can be simplified as

$$e^{iKa} \approx \left(-1 - \pi\Gamma \frac{\delta\omega_B}{\delta\omega_x} \right) \pm i \sqrt{-2\pi\Gamma \frac{\delta\omega_B}{\delta\omega_x} - \left(-\pi\Gamma \frac{\delta\omega_B}{\delta\omega_x} \right)^2} \\ \approx -1 \pm i \sqrt{\left| 2\pi\Gamma \frac{\delta\omega_B}{\delta\omega_x} \right|}. \quad (27)$$

The derivative of Eq. (27),

$$iae^{iKa} dK \approx \pm i \frac{\sqrt{2\pi\Gamma} \frac{\Delta\omega_{xB}}{\delta\omega_x^2} \sqrt{\left| \frac{\delta\omega_x}{\delta\omega_B} \right|}}{2} d\omega, \quad (28)$$

leads to the expressions for the group index,

$$n_g = \frac{c}{v_g} = c \left| \frac{dK}{d\omega} \right| \approx n_b \frac{\sqrt{2\pi\Gamma} \left(\frac{\Delta\omega_{xB}}{\delta\omega_x} \right)^2 \sqrt{\left| \frac{\delta\omega_x}{\delta\omega_B} \right|}}{2\pi} \left| \frac{\omega_B}{\Delta\omega_{xB}} \right|, \quad (29)$$

where we have used $a=\pi c/(n_b\omega_B)$. In the middle of the IB, $|\delta\omega_x/\delta\omega_B|=1$, $|\Delta\omega_{xB}/\delta\omega_x|=2$, one has

$$n_g = n_b \sqrt{\frac{8\Gamma}{\pi}} \left| \frac{\omega_B}{\Delta\omega_{xB}} \right| = \bar{n}_{\text{eff}}. \quad (30)$$

That is, the GVI corresponds to the ECI for $\tau=a$ in the middle of the IB. In Fig. 8, we also plot the GVI as a function of ω , comparing the result rigorously calculated from $n_g=c|dK/d\omega|$ and Eq. (A12) with that from the approximate expression Eq. (29). The two results agree well with each other, and the GVI and ECI curves cross in the middle of the IB.

Since the reflectivity of uniform media are not related to the GVI, even in cases where the GVI differs significantly from the refractive index, it may seem surprising that the reflectivity of the Bragg structure in the middle of the IB is determined by the GVI [see Eq. (30)]. However, a simple and general condition, under which $\bar{n}_{\text{eff}}=n_g$, can be obtained from Eq. (2). Taking the derivative with respect to K on both sides of the equation and using the definition of the GVI, one obtains

$$\omega \frac{\partial \bar{n}_{\text{eff}}}{\partial K} = c \left(\frac{\partial \kappa}{\partial K} - \frac{\bar{n}_{\text{eff}}}{n_g} \right). \quad (31)$$

We see that $\bar{n}_{\text{eff}}=n_g$ if $\omega \partial \bar{n}_{\text{eff}}/\partial K=c(\partial \kappa/\partial K-1)$. A sufficient condition for this is that \bar{n}_{eff} has an extremum (i.e., $\partial \bar{n}_{\text{eff}}/\partial K=0$) and $\partial \kappa/\partial K=1$. According to Figs. 7 and 8 this is the situation encountered in the narrow IB. In other words, $\bar{n}_{\text{eff}}=n_g$ occurs at the extremum of \bar{n}_{eff} . However, we stress that in general the equality of the ECI and the GVI does not necessarily occur at the extremum of the ECI, as additional numerical studies (not shown) have revealed.

5. SUMMARY

We have addressed the problem of high-reflection losses from one-dimensional photonic crystals, using quantum-well Bragg structures as a particular example. We have established the concept of an effective coupling index $n_{\text{eff}}(\omega)$, which is always real for a lossless structure. In calculating the reflection from the boundary of a quantum-well Bragg structure, $n_{\text{eff}}(\omega)$ plays the role for the structure that the usual refractive index would play for a uniform medium, if that boundary is placed half a period from the first quantum well. We consider in detail the special properties of $n_{\text{eff}}(\omega)$ within a spectrally narrow band, called the intermediate band. At such frequencies we can also introduce another effective coupling index, $\bar{n}_{\text{eff}}(\omega)$, which is also real for a lossless structure, and replaces $n_{\text{eff}}(\omega)$ in reflection calculations if the boundary is one period from the first quantum well. The two indices $n_{\text{eff}}(\omega)$ and $\bar{n}_{\text{eff}}(\omega)$ are inversely proportional to each other, and $\bar{n}_{\text{eff}}(\omega)$ has a more direct relation to the group index. Our general approach for identifying effective coupling indices is not restricted to quantum-well Bragg structures, but can be applied to any one-dimensional photonic crystal. In the future, it would be interesting to determine to what extent this approach can be generalized in a useful way to two- and three-dimensional photonic crystals.

APPENDIX A: REVIEW OF BLOCH FUNCTIONS IN QUANTUM WELL BRAGG STRUCTURES

In this Appendix, we review the theory of Bloch functions and photonic band structure of infinitely long quantum-well Bragg structures (Fig. 1). For light propagating along the z direction, with either circular σ^+ or σ^- polarization, the dynamics is governed by Maxwell's propagation equation and the linear semiconductor Bloch equation for the excitonic interband polarization p_m , where m refers to the m th quantum well located at z_m . Detailed discussions can be found, for example, in [7] (see also [5,19–22]). Here we simply write down the solutions of these equations in the frequency domain. Since the thickness of the quantum wells is much less than the spacing between the wells and the wavelength of light, we idealize the quantum wells as infinitely thin. The electric field between two adjacent quantum wells is

$$\begin{aligned}
E(z, \omega) &= E^+(z, \omega) - E^-(z, \omega) = E^+(z_m + \varepsilon, \omega)e^{in_b(\omega/c)(z-z_m)} \\
&\quad - E^-(z_m + \varepsilon, \omega)e^{-in_b(\omega/c)(z-z_m)}, \\
z_m &< z < z_{m+1}, \quad \varepsilon \rightarrow 0^+, \tag{A1}
\end{aligned}$$

with the boundary conditions at each quantum well,

$$\frac{\partial}{\partial z}E(z_m + \varepsilon, \omega) - \frac{\partial}{\partial z}E(z_m - \varepsilon, \omega) = -\frac{4\pi\omega^2}{c^2}\mu\tilde{\phi}(\mathbf{0})p_m(\omega),$$

$$E(z_m + \varepsilon, \omega) - E(z_m - \varepsilon, \omega) = 0, \quad \varepsilon \rightarrow 0^+, \tag{A2}$$

and the excitonic interband polarization given by

$$p_m(\omega) = -\frac{\mu\tilde{\phi}^*(\mathbf{0})}{\hbar} \frac{1}{\omega - (\omega_x - i\gamma)}. \tag{A3}$$

Here, μ is the magnitude of the dipole matrix element of the valence to conduction band transition, γ is the polarization nonradiative decay rate, which throughout this paper is set to zero (ideal quantum-well model), and $\tilde{\phi}(\mathbf{0}) = 2\sqrt{2}/(\sqrt{\pi}a_0)$ (a_0 is the exciton Bohr radius) is the configuration space exciton wave function at zero relative spatial coordinate.

By substituting Eqs. (A1) and (A3) into Eq. (A2), one obtains after some straightforward algebra:

$$\begin{pmatrix} E^+(z_m + \varepsilon, \omega) \\ E^-(z_m + \varepsilon, \omega) \end{pmatrix} = \begin{bmatrix} 1 + \beta & -\beta \\ \beta & 1 - \beta \end{bmatrix} \begin{pmatrix} E^+(z_m - \varepsilon, \omega) \\ E^-(z_m - \varepsilon, \omega) \end{pmatrix}, \tag{A4}$$

with

$$\begin{aligned}
\exp(iK_{\pm}a) &= \frac{[e^{in_b(\omega/c)a}(1 + \beta) + e^{-in_b(\omega/c)a}(1 - \beta)] \pm \sqrt{[e^{in_b(\omega/c)a}(1 + \beta) + e^{-in_b(\omega/c)a}(1 - \beta)]^2 - 4}}{2} \\
&= \text{Re}[e^{in_b(\omega/c)a}(1 + \beta)] \pm \sqrt{\{\text{Re}[e^{in_b(\omega/c)a}(1 + \beta)]\}^2 - 1}, \tag{A9}
\end{aligned}$$

where $K_+ = -K_-$, with the corresponding eigenvectors being

$$\frac{E_0^+(\nu, K_{\pm}; \tau)}{E_0^-(\nu, K_{\pm}; \tau)} = \frac{\exp(iK_{\pm}a) - e^{-in_b(\omega/c)a}(1 - \beta)}{\beta e^{-in_b(\omega/c)a}(1 - 2\tau)}. \tag{A10}$$

Note that while the eigenvectors depend explicitly on τ , the eigenvalues are independent of that quantity. This is expected, since the eigenvalues give the dispersion relations of the bands, which must be independent of the chosen reference point τ in the unit cell.

The Bloch wave function of the quantum-well Bragg structure, in close analog to one-dimensional systems in condensed matter physics, is constructed through the $E_0^+(\nu, K; \tau)$ and $E_0^-(\nu, K; \tau)$ as $u_{\nu, K}(z)e^{iKz}$, where $u_{\nu, K}(z+a) = u_{\nu, K}(z)$, with

$$\beta = -i\Gamma \frac{\omega}{\omega - \omega_x}, \quad \Gamma = \frac{2\pi}{n_b\hbar c} \mu^2 |\tilde{\phi}(\mathbf{0})|^2. \tag{A5}$$

Further taking into account the propagation matrices [see Eq. (A7) below] between adjacent quantum wells gives the unit-cell transfer matrix $\bar{M}(\omega; \tau)$ from $z_m - \tau$ to $z_{m+1} - \tau$, explicitly dependent on τ ($0 \leq \tau \leq a$):

$$\begin{pmatrix} E^+(z_{m+1} - \tau, \omega) \\ E^-(z_{m+1} - \tau, \omega) \end{pmatrix} = \bar{M}(\omega; \tau) \begin{pmatrix} E^+(z_m - \tau, \omega) \\ E^-(z_m - \tau, \omega) \end{pmatrix}, \tag{A6}$$

with

$$\begin{aligned}
\bar{M}(\omega; \tau) &= \begin{bmatrix} e^{in_b(\omega/c)(a-\tau)} & 0 \\ 0 & e^{-in_b(\omega/c)(a-\tau)} \end{bmatrix} \begin{bmatrix} 1 + \beta & -\beta \\ \beta & 1 - \beta \end{bmatrix} \\
&\quad \times \begin{bmatrix} e^{in_b(\omega/c)\tau} & 0 \\ 0 & e^{-in_b(\omega/c)\tau} \end{bmatrix}, \\
&= \begin{bmatrix} e^{in_b(\omega/c)a}(1 + \beta) & -\beta e^{in_b(\omega/c)(a-2\tau)} \\ \beta e^{-in_b(\omega/c)(a-2\tau)} & e^{-in_b(\omega/c)a}(1 - \beta) \end{bmatrix}. \tag{A7}
\end{aligned}$$

The eigenvalues and corresponding eigenvectors of $\bar{M}(\omega; \tau)$ are defined through

$$\bar{M}(\omega; \tau) \begin{pmatrix} E_0^+(\nu, K; \tau) \\ E_0^-(\nu, K; \tau) \end{pmatrix} = \exp(iKa) \begin{pmatrix} E_0^+(\nu, K; \tau) \\ E_0^-(\nu, K; \tau) \end{pmatrix}, \tag{A8}$$

where K is a complex number and ν represents all quantum numbers other than K . The eigenvalues of $\bar{M}(\omega; \tau)$ in Eq. (A8) are given by

$$\begin{aligned}
u_{\nu, K}(z) &= E_0^+(\nu, K; \tau)e^{i(n_b(\omega/c)-K)[z-(z_m-\tau)]} \\
&\quad - E_0^-(\nu, K; \tau)e^{-i(n_b(\omega/c)+K)[z-(z_m-\tau)]} \quad \text{for } z \in (z_{m-1}, z_m), \tag{A11}
\end{aligned}$$

For an infinite structure K must be real on physical grounds, since any finite imaginary part of K would lead e^{iKz} to diverge at $z \rightarrow +\infty$ or $-\infty$. Thus, when K is real, the frequency is within a photonic band; otherwise it is within a bandgap. It is easy to show that in Eq. (A9), K_{\pm} is real (within photonic bands) if and only if $\{\text{Re}[e^{in_b(\omega/c)a}(1 + \beta)]\}^2 - 1 \leq 0$. So for the photonic bands one has

$$\begin{aligned}
\exp(iK_{\pm}a) &= \text{Re}[e^{in_b(\omega/c)a}(1 + \beta)] \pm i\sqrt{1 - \{\text{Re}[e^{in_b(\omega/c)a}(1 + \beta)]\}^2}. \tag{A12}
\end{aligned}$$

In this paper, except where explicitly indicated, all our

discussions are restricted to photonic bands. The eigenvectors in Eq. (A10) and the Bloch wave functions in Eq. (A11) play a crucial role in our definition and analysis of the ECI of the quantum-well Bragg structure.

We finally note two properties of the Bloch function solutions that are useful in the analysis of the ECI, namely,

$$\left[\frac{E_0^+ \left(\nu, K; \tau = \frac{a}{2} \right)}{E_0^- \left(\nu, K; \tau = \frac{a}{2} \right)} \right]^* = \frac{E_0^+ \left(\nu, K; \tau = \frac{a}{2} \right)}{E_0^- \left(\nu, K; \tau = \frac{a}{2} \right)}, \quad (\text{A13})$$

$$\begin{pmatrix} E_0^+(\nu, -K; \tau) \\ E_0^-(\nu, -K; \tau) \end{pmatrix} = -\zeta \begin{pmatrix} E_0^{*-}(\nu, K; \tau) \\ E_0^{+*}(\nu, K; \tau) \end{pmatrix} \quad (\text{A14})$$

$$u_{\nu, -K}(z) = \zeta u_{\nu, K}^*(z), \quad (\text{A15})$$

where ζ is a constant. Equations (A13) and (A14) can be easily proved by substituting Eq. (A12) into Eq. (A10) and comparing the eigenequation (A8) for $\pm K$, respectively. Equation (A15) would be expected by analogy with corresponding expressions in condensed matter physics that follow from time reversal symmetry, and an explicit proof for our problem is obtained by combining Eqs. (A11) and (A14).

ACKNOWLEDGMENTS

We acknowledge financial support from the Defense Advanced Research Projects Agency (DARPA), Office of Naval Research (ONR), Joint Services Optical Program (JSOP), and the Center for Opto-Electronic Devices, Interconnects and Packaging (COEDIP).

REFERENCES AND NOTES

1. J. Joannopoulos, R. Meade, and J. Winn, *Photonic Crystals: Molding the Flow of Light* (Princeton U. Press, 1995).
2. T. Stroucken, A. Knorr, P. Thomas, and S. W. Koch, "Coherent dynamics of radiatively coupled quantum-well excitons," *Phys. Rev. B* **53**, 2026–2033 (1996).
3. M. Hübner, J. Kuhl, T. Stroucken, A. Knorr, S. W. Koch, R. Hey, and K. Ploog, "Collective effects of excitons in multiple quantum well Bragg and anti-Bragg structures," *Phys. Rev. Lett.* **76**, 4199–4202 (1996).
4. J. P. Prineas, C. Ell, E. Lee, G. Khitrova, H. M. Gibbs, and S. W. Koch, "Exciton polariton eigenmodes in light-coupled InGaAs/GaAs semiconductor multiple-quantum-well periodic structures," *Phys. Rev. B* **61**, 13863–13872 (2000).
5. L. I. Deych and A. A. Lisyansky, "Polariton dispersion law in periodic-Bragg and near-Bragg multiple quantum well structures," *Phys. Rev. B* **62**, 4242–4244 (2000).
6. T. Ikawa and K. Cho, "Fate of superradiant mode in a resonant Bragg reflector," *Phys. Rev. B* **66**, 085338 (2002).
7. Z. S. Yang, N. H. Kwong, R. Binder, and A. L. Smirl, "Stopping, storing and releasing light in quantum-well Bragg structures," *J. Opt. Soc. Am. B* **22**, 2144–2156 (2005).
8. Z. S. Yang, N. H. Kwong, R. Binder, and A. L. Smirl, "Distortionless light pulse delay in quantum-well Bragg structures," *Opt. Lett.* **30**, 2790–2792 (2005).
9. A. Andre and M. Lukin, "Manipulating light pulses via dynamically controlled photonic band gap," *Phys. Rev. Lett.* **89**, 143602 (2002).
10. M. F. Yanik and S. Fan, "Stopping light all optically," *Phys. Rev. Lett.* **92**, 083901 (2004).
11. T. Baba and D. Ohsaki, "Interface of photonic crystals for high efficiently light transmission," *Jpn. J. Appl. Phys.* **40**, 5920–5920 (2001).
12. J. Witzens, M. Hochberg, T. Baehr-Jones, and A. Scherer, "Mode matching interface for efficient coupling of light into planar photonic crystals," *Phys. Rev. E* **69**, 046609 (2004).
13. B. Momeni and A. Adibi, "Adiabatic matching stage for coupling of light to extended Bloch modes of photonic crystals," *Appl. Phys. Lett.* **87**, 171104 (2005).
14. Note that in [7] it is called "effective refractive index."
15. M. Born and E. Wolf, *Principles of Optics* (Pergamon, 1980).
16. O. S. Heavens, *Optical Properties of Thin Solid Films* (Dover, 1955).
17. E. D. Palik, *Handbook of Optical Constants in Solids* (Academic, 1985).
18. Note that the last sentence of Appendix A in [7] contains an ambiguous formulation. In the IB, there exists a close relation between n_{eff} and the group velocity index, not the phase index as could be understood from that sentence.
19. L. C. Andreani, "Exciton-polaritons in superlattices," *Phys. Lett. A* **192**, 99–109 (1994).
20. D. Citrin, "Material and optical approaches to exciton polaritons in multiple quantum wells: formal results," *Phys. Rev. B* **50**, 5497–5505 (1994).
21. I. H. Deutsch, R. J. C. Spreeuw, S. L. Rolston, and W. D. Phillips, "Photonic band gaps in optical lattices," *Phys. Rev. A* **52**, 1394–1410 (1995).
22. G. Khitrova, H. M. Gibbs, F. Jahnke, M. Kira, and S. W. Koch, "Nonlinear optics of normal-mode coupling semiconductor microcavities," *Rev. Mod. Phys.* **71**, 1591–1639 (1999).